Tight binding molecular dynamics study of ni clusters. Journal of Chemical Physics, 104, 992

ARTICLE *in* THE JOURNAL OF CHEMICAL PHYSICS · JANUARY 1996

Impact Factor: 2.95 · DOI: 10.1063/1.470823

Tight binding molecular dynamics study of Ni clusters

N. N. Lathiotakis
Institute of Electronic Structure and Laser, Foundation for Research and Technology—Hellas, P.O. Box 1527, Heraklio, Crete, Greece 71110 and Department of Physics, University of Crete, P.O. Box 1470, Heraklio, Crete, Greece 71409

A. N. Andriotis
Institute of Electronic Structure and Laser, Foundation for Research and Technology—Hellas, P.O. Box 1527, Heraklio, Crete, Greece 71110

M. Menon[a)]
Department of Physics and Astronomy, University of Kentucky, Lexington, Kentucky 40506-0055 and Center for Computational Sciences, University of Kentucky, Lexington, Kentucky 40506-0045

J. Connolly
Center for Computational Sciences, University of Kentucky, Lexington, Kentucky 40506-0045

(Received 31 July 1995; accepted 9 October 1995)

A minimal parameter tight binding molecular dynamics scheme is used to study Ni_n clusters with $n \leqslant 55$. We present theoretical results for relaxed configurations of different symmetries, binding energies, and normal vibrational frequencies for these clusters. Our results are in good agreement with experiment and previous theoretical predictions. We also compare relative stabilities of fcc structures with icosahedral structures. In particular, we find that for clusters whose size allows them to form a close icosahedral geometry (normal or twinned), the closed icosahedral structures yield larger binding energies than fcc structures. The fcc structures, in turn, are found to be more stable than open icosahedral structures for $n \leqslant 55$. Additionally, results for normal vibrational frequencies and ionization energies for $n \leqslant 10$ are also presented. The present results, along with previous successful applications of the method on semiconductor systems, indicate that tight-binding molecular dynamics scheme can be relied on to provide a useful semiempirical scheme in modeling interactions in both covalent and metallic systems. © *1996 American Institute of Physics.* [S0021-9606(96)00403-6]

I. INTRODUCTION

Motivated by the success of the tight-binding molecular dynamics (TBMD) scheme in the treatment of semiconductor systems,[1–6] we extend the method to treat transition metals, transition metal alloys, and transition metal impurities in semiconductors. The goal is to develop an efficient methodology, which is computationally fast and sufficiently flexible enough to accurately reproduce known properties when applied to both covalent and metallic systems. The generalization requires the incorporation of *d* orbitals in the construction of the TB Hamiltonian and the availability of sufficient experimental or accurate first principles theoretical results to be used as a guide in obtaining the parameters. It should be noted that such a general theory must contain only a minimal parameter set in order to be applicable to a wide range of systems. Once an accurate fitting is achieved for small systems, the quantum mechanical nature of the TB theory ensures reliable scalability for arbitrary sizes, including bulk materials. As evidenced by our earlier results, such a theory can be relied on to successfully bridge the gap between the accurate *ab initio* methods that demand excessive computational work and the existing empirical methods. Thus, the proposed method can serve as an efficient tool for studying complex systems for which *ab initio* methods are not easily applicable. As will become clear in the following, the method can take a firm *ab initio* character with no adjustable parameters, depending on the level of accuracy in combination with the computational efficiency required.

The first application of our general TB-MD method was to clusters of transition metal atoms. These systems are challenging because of the rapid change, in coordination with cluster size. Recent advances in experimental techniques have resulted in a wealth of data for nickel,[7–11] cobalt,[11,12] iron,[9,11] copper,[10,13] gold,[14,15] and platinum[16] clusters. These results reveal an evolutionary process taking place for the clusters as the cluster size increases and reaches the bulk limit. For example, for fcc materials, it appears that the fcc structure seems to be attained for clusters of very large size, while smaller clusters tend to exhibit geometries based on the icosahedral (IC), or the cuboctahedral (CO),[7,11,12] structures. Although this trend has been observed for cluster sizes with the number of atoms $n > 55$, the experimental results cannot determine with certainty the geometry of smaller clusters (with $n < 55$) for which the IC geometry is predicted to be most preferable.[7,11]

A comparison of the experimental results for transition metal clusters (TMCs) with those for clusters of simple metal atoms reveals that while the latter give evidence for the existence of ''magic numbers,'' no such reference is made for the former. This lack of the existence of ''magic numbers'' in TMCs was attributed to the fact that the usual preparation

[a)]Corresponding author: e-mail: super250@convex.uky.edu

 0021-9606/96/104(3)/992/12/$6.00

TABLE I. Summary of results for binding energy per atom and the average bond length (r_e) using *ab initio* methods.

Cluster		r_e(Ni–Ni) (Å)	*BE*/*N* (eV/atom) Basch *et al.* (*) (Ref. 19)	Tomonari *et al.* (Ref. 20)	Mlynarsky *et al.* (Ref. 21)	Gropen *et al.* (Ref. 22)	Rösch *et al.* (**) (Ref. 23)
Ni_2		2.24±0.04 exp[a]	0.933 exp[a]				
		2.33 (SCF) (Ref. 19)	0.457	0.238 (SCF)[b]			
		2.33 (CI) (Ref. 19)	0.713	1.390 (CI)[b]			
		2.03 (LDA) (Ref. 21)			1.820		
		2.11 (NL) (Ref. 21)			1.440		
Ni_3	($D_{\infty h}$)	2.38	0.508				
	(D_{3h})	2.492	0.452	0.193 (SCF)			
Ni_4	($D_{\infty h}$)	2.492	0.578				
	(D_{4h})	2.492	0.582	0.504 (SCF)			
	(T_d)	2.492	0.323		2.99 (LDA)		
					2.27 (NL)		
		2.232			3.35 (LDA)		
		2.359			2.27 (NL)		
	(D_{2h})	2.49 (Ref. 26)					
Ni_5	(C_{4v})	2.492	0.708	0.502 (SCF)	3.28 (LDA)		
					2.63 (NL)		
	(C_{2v})	2.49 (Ref. 26)					
Ni_6	(O_h)	2.49	0.725	0.522 (SCF)		0.380(****)	2.29
		2.28(**)					2.48
	(C_{5v})	2.49 (Ref. 26)					
Ni_7	(D_{5h})	2.49[26] (Ref. 26)					
Ni_8	Cube	2.49					2.45
		2.19(**)					2.84
	S_4	2.49 (Ref. 26)					
Ni_{19}	fcc	2.49					3.51
		2.34(**)					3.66
Ni_{44}	fcc	2.49					4.28
		2.36(**)					4.40
Ni bulk	fcc	2.492					4.44 exp[c]
		2.45					5.62 (LDA) (Ref. 44)

(*) SCF-ECP (**) Optimized geometry (***) LCGTO/LDF (****) CASSCF

[a]Quoted in Ref. 19.
[b]At an experimental bond length of 2.3 Å reported in Ref. 25.
[c]Quoted in Ref. 23.

technique of laser vaporization in a flow system for TMCs involves cluster growth far from equilibrium.[7,12] Recently, however, the mass distribution of various TMCs analyzed with a near threshold photoionization experiments and time-of-flight mass spectroscopy[11] has indicated strong effects at cluster sizes for $n=55$, 147, 309, and 561 atoms. These effects were attributed to closed IC geometry possible for these size clusters. Several noticeable effects at intermediate cluster sizes were assigned to a cluster growth, in accordance with the "umbrella model."[11,17,18]

From the theoretical point of view, most of the *ab initio* calculations on TMCs have been performed within the local density approximation (LDA),[19–27] because the size and the complexity of the transition metal atoms do not allow a Configuration Interaction (CI) approach to TMCs. For this reason, the CI calculations are usually restricted only to the dimer,[19,20] and very often the level of the CI calculation achieved is crucial in determining the ground state of a transition metal atom and/or dimer. Thus, the results of the *ab initio* calculations fail to agree among themselves. In Table I, we have summarized *ab initio* results for Ni_n clusters for which we have applied our TBMD method. Also, in the same table, the methods used are listed along with the results for binding energy (BE) per atom and the average bond length, r_e.

Most of the theoretical calculations for Ni_n clusters rely on cluster geometries chosen *a priori*,[19–23,26] assuming bulk Ni interatomic distance, i.e., 2.49 Å, for bond lengths. Sometimes a symmetry restricted geometry optimization is attempted, which usually results in significantly different bond lengths.[21–23,26] More recently, there have also been a few calculations reported for which Jahn–Teller distortions and/or partial geometry optimizations have been considered, especially for small clusters[19–22,28] ($n\leqslant 6$). These optimiza-

tions reveal the Jahn–Teller distortions to have a significant effect on cluster properties. Full geometry optimization has only recently become tractable with the use of simulations based on molecular dynamics.

For large Ni_n clusters there is, to our knowledge, only one reported calculation,[29] which is based on the molecular dynamics and the embedded atom many-body potential method. In that work, Cleveland and Landman[29] found that Ni clusters undergo a nondiffusive transformation from the CO to the IC structure upon heating. Similar findings were reported by Valkealahti and Manninen[30] for copper clusters from results based on the effective medium theory.

Recently, we performed calculations[31,32] on Ni_n clusters with $n \leqslant 55$ using, for the first time, the tight-binding molecular-dynamics (TBMD) scheme, which allows full geometry optimization with no symmetry constraints. Our results led us to the following conclusions for these clusters.

(i) The IC geometry is preferable for clusters that can form closed icosahedral structures.

(ii) The fcc clusters, based either on cuboctahedral (CO) geometry or the Wulff-polyhedron, are more stable than the open icosahedral (IC) structures.

Our conclusions were based on results of geometry optimizations with initial configurations that consisted of Mackay's[33] icosahedra, Wulff's polyhedra,[34] CO geometry[35] and open IC structures derived from the "umbrella model"[11,17,18] of cluster growth.

Within the range of geometries considered, the IC structure was found to be energetically most favorable for Ni_n with $n=13$ and 55 atoms, i.e., for clusters that can form one of Mackay's icosahedra. For all other values of $n \leqslant 55$, the cluster geometries based on fcc crystal structures were found energetically more favorable.[32] Thus, our results for the IC closed shell clusters are in agreement with other reported calculations[29] and the experimental data.[7–11]

We, however, find no theoretical results discussing the stability of Ni clusters with open IC structure, while the experimental results[7–11] for these clusters (with $n \leqslant 55$) are not conclusive. It appears that for small Ni clusters ($n \leqslant 55$ and $n \neq 13,55$) the CO structures should not be ruled out as stable low-energy geometries whenever it is not possible to form closed IC geometry. Furthermore, our recent investigations indicate that in the range $n \in [2-55]$ atoms, in addition to the closed IC clusters with $n=13,55$, additional closed shell IC structures can be obtained for twin-icosahedral structures considered by Farges *et al.*[36] for $n \leqslant 55$. In view of this, an investigation is worthwhile to determine if the twin-IC structures follow our predicted trends for cluster stability, i.e., if it is more stable than the fcc based structures.

In the present paper we expand our investigation by including clusters exhibiting twin IC geometries for a systematic stability study and compare these results with our previous conclusions. Additionally, we also report theoretical results for normal frequencies using our TBMD scheme. After giving a brief summary of the basic ingredients of our approach in the next section, we proceed with the presentation of our new results and conclusions in Secs. III and IV, respectively.

II. METHOD

The TBMD method involves the following calculational steps.

(i) Construction of the TB Hamiltonian from which the electronic eigenstates and eigenvalues are calculated. This must include an efficient scaling scheme for the Slater–Koster (SK) TB matrix elements to ensure satisfactory transferability.

(ii) Calculation of the total energy of the system and, from it, the calculation of the forces acting on each atom of the system.

(iii) Full geometry optimization of the system by following its time evolution starting from specific initial geometries.

A. Construction of the TB Hamiltonian

In constructing the TB Hamiltonian, we assume an orthogonal atomic basis set. The details of the method with applications to semiconductor systems is discussed in Ref. 1. The diagonal matrix elements of the TB Hamiltonian (atomic term values) are taken to be configuration independent and equal to the values given in Ref. 37 (Solid State Table, and p. 484). The off-diagonal matrix elements are taken to have a Slater–Koster-type angular dependence with respect to the interatomic separation vector,[38] and scaled exponentially with respect to the interatomic distance r:

$$V_{\lambda\lambda'\mu} = V_{\lambda\lambda'\mu}(d) S(l,m,n) \exp[-\alpha(r-d)], \tag{1}$$

where d is the equilibrium bond length in the corresponding bulk material, S is the Slater–Koster-(SK) type function of the direction cosines l, m, n of the separation vector $\mathbf{r}$, and α is an adjustable parameter. We follow Ref. 1 and take $\alpha = 2/d$. We use a smooth Fermi-type function to cut off interactions between atoms separated by large distances, ensuring that the average cutoff distance r_c is between the nearest and next-nearest neighbors in the bulk solid. We further check for the convergence by varying this cutoff distance within a certain range, to ensure that the results are unaffected. In particular, we find a good choice for the cutoff distance to be $r_c = 3$ Å.

The exponential scaling scheme, used here, appears to be more appropriate than Harrison's d^{-2} for interatomic distances that deviate from equilibrium bulk distances, where Harrison's scheme is applicable. This can be justified by the exponential behavior of the atomic wave functions far from the atomic nucleus, indicating that an exponential scaling should be more appropriate. This has been verified by two of the authors in a previous work,[39] employing *ab initio* total energy calculations on Si clusters in the restricted Hartree Fock approximation. Additionally, recent investigations by Andriotis[40] have shown that as long as the system remains in phases of constant electron density, the diagonal matrix elements can be, to a very good approximation, taken independent of the local environment, but the off-diagonal elements exhibit a strong dependence on the number of nearest neighbors. Therefore, while our assumption of keeping the on site SK-TB matrix elements to be constants is justified, further

TABLE II. Universal constants, on site energies and the parameter r_d, for Ni used in the present work.

Parameter	Value
r_d	0.71 Å
E_s	−18.90 eV
E_p	100.00 eV
E_d	−18.90 eV
$\eta_{ss\sigma}$[a]	−0.47
$\eta_{sp\sigma}$	1.84
$\eta_{pp\sigma}$	3.24
$\eta_{pp\pi}$	−0.81
$\eta_{s\,d\sigma}$	−3.16
$\eta_{p\,d\sigma}$	−2.95
$\eta_{p\,d\pi}$	1.36
$\eta_{d\,d\sigma}$	−16.20
$\eta_{d\,d\pi}$	8.75
$\eta_{d\,d\delta}$	0.00

[a]This value is not taken from the solid state table of Ref. 37, but rather from p. 484, Eq. (20-7), and it is better suited for the band structure calculation for Ni.

investigation is needed to determine any error that can be introduced by assuming a form of scaling, that does not explicitly include local lattice field effects.

It seems that for large Ni clusters for which the cluster stability is mainly an interplay between two mutually competing closed packed structures, our scaling form of Eq. (1) is adequate. For small clusters ($n \leqslant 10$), however, it will be interesting to see if the results are affected by a more accurate scaling scheme. Such investigations are currently in progress. For the present calculations we follow our previous calculational scheme,[31,32] and assume that the values of the parameters $V_{\lambda\lambda'\mu}(d)$ can be expressed in terms of the universal constants $\eta_{\lambda\lambda'\mu}$ of Ref. 37:

$$V_{\lambda\lambda'\mu} = \eta_{\lambda\lambda'\mu} \frac{\hbar r_d^{\tau}}{m d^{\tau+2}}, \tag{2}$$

where r_d is a characteristic length for each transition metal. The parameter $\tau=0$ for $s-s$, $s-p$, and $p-p$ interactions, $\tau=3/2$ for $s-d$, and $p-d$, $\tau=3$ for $d-d$ interactions.

In Table II we present the universal constants $\eta_{\lambda\lambda'\mu}$, the on-site energies E_s, E_p, E_d, and the parameter r_d for Ni. The SK-TB matrix elements derived using the constants of Table II results in a band structure for Ni given by Harrison.[37] It should be noted that the large positive value of E_p in Table II is to merely suppress the effect of $3p$ orbitals in Harrison's approximations for the band structure of transition metals. On the other hand, due to the poor description for the s band within the LCAO approximation, the on-site energies of the $4s$ and $3d$ orbitals are taken to be the same, with a simultaneous change of the $\eta_{ss\sigma}$ constant. The latter is determined by fitting to the band structure at Γ.

The universal constants $\eta_{\lambda\lambda'\mu}$ used here, although capable of producing the correct band structure, are limited in the extent of transferability, which may become pronounced when applied to clusters of small size ($n<10$). This is because the free atom energy levels cannot be described with the constants of Table II, and as a result, the eigenvalues of the molecular orbitals of the small clusters will not be calculated correctly. Fortunately, this drawback is to a large extent eliminated through the adjustable parameter ϕ_0 in our approach (which is determined by fitting the results in the dimer regime) and does not appreciably affect the stability studies. It will, however, affect results that do not explicitly include the repulsive interaction terms. For example, ionization energies of small clusters is not expected to be quantitatively correct, while the opposite is expected to be true for the stable configurations and the vibrational frequencies of the clusters.

Using the universal constants of Table II, we proceed with the construction of the cluster Hamiltonian, H, in real space according to Eqs. (2) and (1). The matrix element H_{ij} of this Hamiltonian refers to the pair of atoms i and j of the cluster. Each atom is represented by a 10×10 block with respect to the orbital basis set $|s\rangle$, $|p_i\rangle$, $|d_i\rangle$, and $|s^*\rangle$, where $|s\rangle$ stands for the s orbital, $|p_i\rangle$ for the three p orbitals, $|d_i\rangle$ for the five d orbitals, and $|s^*\rangle$ for the excited s orbital. Thus, for an n atom cluster, the Hamiltonian H is a $10n \times 10n$ matrix,

$$H = \begin{pmatrix} H_{11} & H_{12}\cdots & H_{1n} \\ H_{21} & H_{22}\cdots & H_{2n} \\ \vdots & \vdots & \vdots \\ H_{n1} & H_{n2}\cdots & H_{nn} \end{pmatrix}, \tag{3}$$

with

$$H_{ij} = \begin{pmatrix} H_{ss}^{(ij)} & H_{sp_x}^{(ij)} & H_{sp_y}^{(ij)} & H_{sp_z}^{(ij)} & H_{sd_{xy}}^{(ij)} & \cdots H_{ss^*}^{(ij)} \\ H_{p_x s}^{(ij)} & H_{p_x p_x}^{(ij)} & H_{p_x p_y}^{(ij)} & & & \\ \vdots & \vdots & \vdots & \vdots & \vdots & \vdots \end{pmatrix}. \tag{4}$$

The eigenvalues, ϵ_i, and their corresponding eigenvectors, $|c_i\rangle$, of the cluster Hamiltonian are then obtained by solving the eigenvalue equation,

$$H|c_i\rangle = \epsilon_i|c_i\rangle. \tag{5}$$

Next, we describe the evaluation of the total energy of the cluster and interatomic forces from it.

B. Calculation of total energy and atomic forces

In the tight-binding scheme, the total energy, U, can be written as a sum of three terms:

$$U = U_{\rm el} + U_{\rm rep} + U_{\rm bond}. \tag{6}$$

The term, $U_{\rm el}$ (electronic part) is given by summing over the eigenvalues ϵ_k of the one electron occupied states of the tight-binding Hamiltonian, given by Eqs. (3)–(5), i.e.,

$$U_{\rm el} = \sum_{k}^{\rm occ} \epsilon_k \theta_k, \tag{7}$$

where θ_k is the occupation number of the kth state.

The second term of Eq. (6), $U_{\rm rep}$, is a repulsive term that includes contributions from ion–ion repulsion interactions and a correction to the double counting of the electron–electron interactions in the first term, $U_{\rm el}$. Here $U_{\rm rep}$ is given by a sum of short-ranged repulsive pair potentials, ϕ_{ij}, and taken to scale exponentially with interatomic distance:

$$\phi_{ij}(r_{ij})=\phi_0\ \exp[-\beta(r-d)], \tag{8}$$

where we take $\beta=4\alpha$. The value of ϕ_0 is fitted to reproduce the correct experimental bond length for the Ni dimer (2.20 Å[19]). We obtain a value of 0.367 eV for ϕ_0. The cutoff distance used (3.0 Å) for the repulsive term is taken to be the same as the one used for the attractive electronic term. The use of a spherically symmetric function for the pair potential can be justified by the fact that this functional form is known to give good results for semiconductor compounds, which contain strongly directed bonds. Therefore, it is expected to be even more valid for metallic bonds, where the directionality of the bonds is generally less pronounced.

The third term, $U_{\rm bond}$, is a coordination-dependent correction term to the total energy. It is needed because the first two terms of Eq. (6) are not sufficient to exactly reproduce cohesive energies of dimers through bulk structures. It was introduced by Tomanek and Schluter,[41] and its presence enables one to bring cohesive energies of clusters of arbitrary sizes in agreement with *ab initio* values. It should be noted, however, that only the first two terms $U_{\rm el}$ and $U_{\rm rep}$ contribute to the interatomic forces; the $U_{\rm bond}$ term is added at the end of the calculation, after the relaxation has been obtained. It is a significant term, however, as it distinguishes various isomers for a given cluster size. The coordination-dependent term is

$$U_{\rm bond}=n[a(n_b/n)^2+b(n_b/n)+c], \tag{9}$$

where n_b is the number of bonds and n is the number of atoms of the cluster. Since we use a smooth function for the cutoff distance for the interactions, we can determine the number of bonds using

$$n_b=\sum_i\left[\exp\left(\frac{r_{ij}-R_c}{\Delta}\right)+1\right]^{-1}, \tag{10}$$

where the sum is over all bonds in the cluster. This term takes into account the number of bonds formed in the cluster. The parameters a, b, c are obtained by fitting $U_{\rm bond}$ to *ab initio* results for three clusters of different sizes according to the equation

$$U_{\rm bond}=U_{ab\ initio}-U_{\rm el}-U_{\rm rep}. \tag{11}$$

Thus, there are four adjustable parameters in our scheme [a, b, c from Eq. (9) and ϕ_0 from Eq. (8)]. These parameters, once adjusted to reproduce known results (theoretical or experimental) for small clusters, are then kept fixed in subsequent calculations for clusters of arbitrary sizes. We take $R_c=3.0$ Å and $\Delta=0.1$ Å. In order to determine the parameters a, b, and c, we used the experimental binding energy of the dimer (0.93 eV/atom[19]) and the *ab initio* results for Ni_6 and Ni_8 in Ref. 23. This gave $a=0.052$ eV, $b=0.213$ eV, and $c=-0.509$ eV.

As stated previously, the evaluation of the interatomic forces involves the energy terms $U_{\rm el}$ and $U_{\rm rep}$ only. In particular, the force $\mathbf{f}_i$ acting on the ith atom is

$$\mathbf{f}_i=-\frac{\partial}{\partial\mathbf{r}_i}(U_{\rm el}+U_{\rm rep}). \tag{12}$$

The simple analytic form of $U_{\rm rep}$ [Eq. (8)] makes the evaluation of $-\partial U_{\rm rep}/\partial\mathbf{r}_i$ rather straightforward. The contribution to the force $\mathbf{f}_i$ from $U_{\rm el}$, however, requires the use of the Hellmann–Feynman theorem,

$$\frac{\partial\epsilon_k}{\partial\mathbf{r}_i}=\langle c_k|\frac{\partial H}{\partial\mathbf{r}_i}|c_k\rangle. \tag{13}$$

The spatial derivative of the Hamiltonian appearing in Eq. (13) is obtained by taking the spatial derivative of the matrix elements of Eqs. (3) and (4). This task is made easier by the simple exponential scaling of the SK-TB matrix elements with the interatomic distances [Eq. (1)] and the simple algebraic form of the functions $S(l,m,n)$.

Molecular dynamics can now be performed by numerically solving Newton's equation for each component of the force,

$$m\frac{d^2x}{dt^2}=f_{ix}, \tag{14}$$

to obtain the coordinates as a function of time. A small damping force is added to simulate energy loss for reaching the equilibrium configuration for the cluster. Many widely differing initial geometric configurations are considered in the simulations. The final equilibrium configurations thus obtained correspond to local minima of the total energy. Our goal is to identify the cluster configuration corresponding to the absolute minimum of the total energy. For small clusters this is easily achieved. For large clusters, however, a full configurational search is computationally prohibitive. Instead, for these clusters, we use clues from experimental and theoretical evidences to construct initial geometries and then perform a full symmetry unrestricted optimization. Although such an approach is quite efficient, it can still leave some cluster configurations that could contain the most stable geometry.

C. Normal vibrational modes

The normal frequencies of the clusters can be evaluated from the eigenvalues of the Dynamical Matrix, D, defined as

$$D_{ij}=\frac{\partial^2U}{\partial x_i\,x_j}, \tag{15}$$

where x_i and x_j are the cluster coordinates.

For a cluster with number of atoms n, we have $3n$ degrees of freedom, resulting in $3n$ eigenvalues. Six of them (five for linear structures) should be zero, corresponding to the free translation and rotation of the cluster. The existence of negative eigenvalues means that the corresponding cluster structure does not correspond to a minimum of the total energy, but rather a saddle point.

The dynamical matrix for this work was evaluated numerically, i.e., by taking small displacements from the equilibrium point.

D. Calculation of ionization energies

The ionization energy for the cluster of atomic population n is defined as the energy difference, ΔE_n, of the energy, $E_n^{(0)}$, of the neutral cluster from the energy E_n^+ of the same cluster with one electron removed, i.e.,

$$\Delta E_n = E_n^+ - E_n^{(0)}. \tag{16}$$

In obtaining E_n^+, we further relax the neutral cluster configuration after removing the electron. According to Koopman's theorem, one expects the ionization energy ΔE_n to start from a value approximately equal to the highest occupied (molecular) orbital energy in the case of small clusters and approach the value of the work function of the system as $n \to \infty$. The variation of the ionization energy with the cluster size may be not monotonic, due to major changes in the structure of the cluster as its size increases. Such a behavior is expected for small paramagnetic TMCs, while for large clusters a gradual variation of the ionization energy is expected as their atomic population increases. In the latter case both theory and experiment indicate a rather smooth cluster growth based on the "umbrella model"[17,18] for IC packing.

Within the approximations of our TBMD calculational scheme, we can only check the qualitative behavior of the ionization energy. This is because the set of SK-TB parameters we are using implies that the expected ionization energy for small clusters to be (by Koopman's theorem) approximately equal to the on-site energy $E_s = E_d$ (which is usually much larger than the highest occupied s-orbital energy of the free atom). Nevertheless, a calculation of the ionization energies according to Eq. (16) within the present calculational scheme, will allow us not only to follow its variation with the cluster size, but also to point out the inherent limitations of the present application of our TBMD calculational scheme. It is worth noticing that these limitations arise mainly from the choice of the SK-TB parameters and the extent of their transferability. Possible improvements of the present scheme are discussed in Sec. IV.

III. RESULTS AND DISCUSSION

A. Geometry optimization and stability

We have applied our TBMD scheme to Ni clusters (Ni_n) for $n \leqslant 55$ atoms. Since the present scheme imposes no *a priori* symmetry restrictions, we can perform full optimization of cluster geometries. For small clusters (i.e., for $n \leqslant 10$), we were able to to perform a full configurational space search to determine the lowest-energy configurations, and our results are extensively discussed in Ref. 31. In Table III we list the binding energies and average bond lengths for Ni clusters with $n \leqslant 10$. Our results led us to two important conclusions:[31] The first being that Jahn–Teller distortions play a dominant role in cluster geometry, and should not be neglected from any realistic calculations. The second conclusion refers to our observation about the increased relative stability of the octahedral (or fcc-like) structures in small clusters. In particular, for $n \geqslant 6$ and up to ten atoms, octahedral structures are most stable with the exception of Ni_7, for which the pentagonal bipyramid is lowest in energy. It should, however, be noted that the pentagonal bipyramid is approximately a half-icosahedron that can be formed for $n = 13$ (we will refer to that later). The present calculations seek to determine if our second conclusion is inherently related to the choice of the SK-TB parameters, which in turn have been obtained by fitting only to the band structure of the bulk material.

TABLE III. Binding energies and average bond lengths for Ni clusters with $n \leqslant 10$.

Cluster		Binding energy	$\langle r_e \rangle$
n	Symm.	eV/atom	Å
2		0.93 (0.93[a])	2.20
3	D_{3h}	1.66	2.30
4	D_{4h}	1.87	2.26
5	T_d	2.16	2.42
6	D_{4h}	2.36	2.47
7	D_{5h}	2.42	2.51
8	C_{2h}	2.45	2.50
9	C_s	2.53	2.46
10	T_d	2.72	2.50

[a]Reference 19.

For larger clusters ($10 \leqslant n \leqslant 55$), a full configurational search is not possible with the available computational resources. Instead, led by the experimental and theoretical results on small clusters, we examined cluster structures of various symmetries for each size. In the following, we discuss our choice for initial geometries and the resulting final structures in more detail.

It is clear that there are many ways to arrange atoms to form octahedral structures. For example, starting from the smallest octahedron, Ni_6 [Fig. 1(a)], one can easily build the second multioctahedron with $n = 19$, having three atoms on each side. Similarly, the third multioctahedron with $n = 44$ can be constructed by surrounding Ni_6 with layers of atoms.

Now, if we cut apex atoms of a multioctahedral structure symmetrically, we can construct a Wulff polyhedra [Fig. 1(b)] or the cuboctahedra [Fig. 1(c)], which can also be considered as a special case of Wulff polyhedra. For example, by removing the six apex atoms from the 19-atom octahedron,

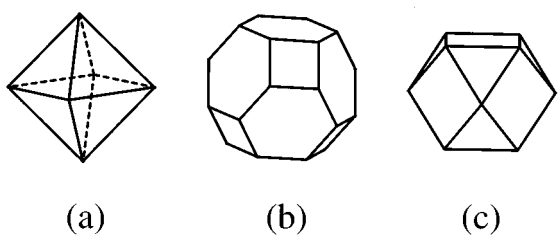

FIG. 1. (a) Octahedron, (b) Wulff's polyhedron, and (c) cuboctahedron.

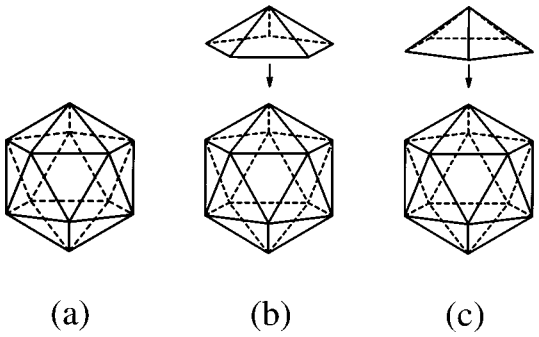

FIG. 2. (a) Mackay's icosahedron, (b) IC1-type cluster growth, and (c) IC2-type cluster growth.

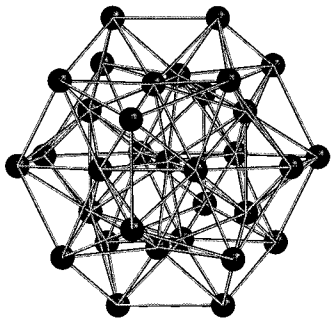

FIG. 3. The twin-icosahedral structure for $n=33$ atoms.

we get the Ni_{13} cuboctahedron. Mackay's icosahedra[33] are constructed similarly i.e., by expanding the first icosahedron for $n=13$ [Fig. 2(a)], (by doubling all the bonds and placing extra atoms at the bond centers so that bond lengths remain unchanged).[33] Thus, Ni_{55}, which is the second Mackay's icosahedron, contains the first icosahedron (Ni_{13}) as a core. We call these two structures ''closed icosahedral.'' There are two ways to construct other icosahedral structures for $13<n<55$. The first method involves adding six-atom caps (or ''umbrella'') to the first icosahedron in an ''eclipsed position'' with respect to the top pentagon of the initial icosahedron [Fig. 2(b)].[7] We call this configuration IC1. The second method consists of adding six-atom caps in ''staggered position'' (rotated by 36°) with respect to the top pentagon of the initial icosahedron [Fig. 2(c)], so that the final structure forms a part of the second Mackay's icosahedron. We call this the IC2 configuration. Both methods describe the type of cluster growth known as the ''umbrella model.''[17,18] Using the latter approach, one can reach the second closed icosahedron, starting from the first Mackay's polyhedron, when all possible caps are included.

We call all the intermediate geometries ''open'' icosahedral structures.[33] There is yet another class of geometries based on the icosahedron, namely the twin icosahedral structures considered by Farges *et al.*[36] These structures are constructed from the 13-atom icosahedron if one adds atoms by reflecting the central atom off each face of the 13-atom icosahedron. If all the reflections are considered, a closed structure can be constructed for $n=33$ (Fig. 3), which consists of a dodecahedron surrounding the initial icosahedron.

For $n=13$ we have considered two geometries: (i) First Mackay's icosahedron [Fig. 2(a)],[33] and (ii) the first cuboctahedron [Fig. 1(c)]. The latter is a fcc-like structure based on an octahedron. It consists of a central atom and its 12 first neighbors in a fcc packing structure. The relaxed Mackay's icosahedron (Fig. 4) is found to be lower in energy over the cuboctahedral configuration. Despite the Jahn–Teller distortions, the IC structure is almost unchanged after relaxation, while the fcc-like structure is fully distorted. Interestingly, the octahedral structure examined for Ni_{14} (i.e., the conventional cell for fcc, which can also be imagined as an octa-capped octahedron) was found stable, and with hardly any distortions. We found the Ni_{13} IC structure to have larger binding energy per atom, even when compared to the Ni_{14} octahedral structure.

For $n=19$ we compare the stability of the second multioctahedral structure (which is identical to the structure obtained if we add the second neighbors to the Ni_{13} cuboctahedron), with three open IC structures produced using the three proposed constructions. The first of these (IC1 type) can be thought of as made up of two interpenetrating icosahedra (though not exactly). The second one can be thought of as a pentagonal bipyramid sitting over an icosahedron, with its ring atoms exactly above the upper waist atoms of the icosahedron (the IC2 type). The third of these is an open twin-icosahedral structure, constructed by the reflections of the central atom over six of the faces of the initial icosahedron. These three relaxed structures were found to be almost isoenergetic with each other (their total energies differ only by ≈ 0.05 eV per atom, with the first structure being lowest in energy among the three). But the fcc structure was found to be the most stable, with its binding energy being 0.7 eV per atom more than the first icosahedral structure. The fcc structure was also the least distorted, while the icosahedral structures showed considerable distortions, particularly the first (IC1 type). We show the relaxed configuration for the multioctahedral Ni_{19} cluster in Fig. 5.

For $n=23$ we compare the stability of the fcc double conventional cell [Fig. 6(a)] with an IC1-type icosahedral structure [Fig. 6(b)], obtained by adding two six-atom caps

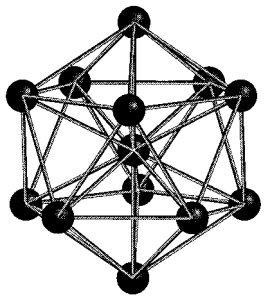

FIG. 4. The relaxed geometry for the icosahedral Ni_{13}.

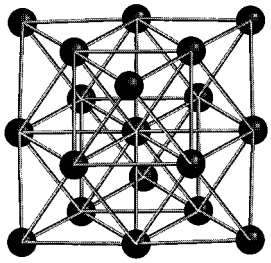

FIG. 5. The relaxed geometry for the fcc (multioctahedral) Ni_{19}.

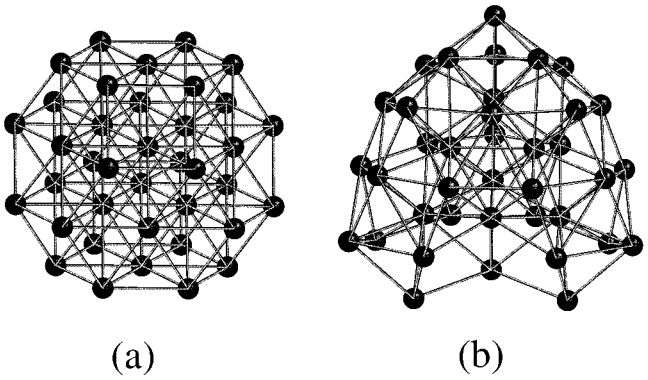

FIG. 7. Geometries of the relaxed (a) fcc (Wulff polyhedron) and (b) icosahedral (IC2) clusters for $n=38$ atoms.

to the IC Ni_{13} and over two neighboring atoms, so that two atoms of the one cap coincide with two atoms of the other cap. Here again, the fcc structure is energetically more favorable. This is also the case for Ni_{24}, where an IC2-type icosahedral structure is compared with a fcc structure, the latter being more stable energetically.

For $n=33$ we find the twin closed icosahedron to be very stable. This is an interesting case because it serves as a check of our predictions when compared to previous findings.[31,32] In particular, we find that clusters with closed IC geometries are more stable than fcc structures, while clusters with open IC geometries are less stable than fcc structures. The cluster Ni_{33} can form a closed IC structure, namely the twin-IC one considered by Farges *et al.* On MD simulation we find that it relaxes with little distortion into a perfect twin-IC structure with much greater binding energy than any other geometry considered for this cluster (fcc or open-IC types). Thus, the present results for Ni_{33} are in good agreement with previous predictions.

In the case of $n=38$, we can construct a fcc structure by removing the six apex atoms from the third ($n=44$) multioctahedron. The structure thus obtained is a Wulff polyhedron [Fig. 7(a)]. One can also construct an icosahedral structure of the IC2 type [Fig. 7(b)] by adding five caps to Ni_{13}. The relaxed fcc structure is found to be more stable than the IC2.

For $n=43$, we examine the stabilities of two fcc structures constructed in different ways. The first geometry is obtained by surrounding the central atom with its neighbors up to the third shell [Fig. 8(a)], while the second structure is obtained from the Ni_{44} octahedron by removing one of its six farthest atoms from the center [Fig. 8(b)]. The latter geometry is found to be more stable with binding energy 0.14 eV per atom larger than the former. Interestingly, the second geometry has a smaller binding energy, even when compared with the Ni_{38} fcc structure (which is a Wulff polyhedron).

Ni_{55} provides an interesting case, where stability comparison can be made between the second Mackay's icosahedron [Fig. 9(a)] and the fcc cuboctahedron [Fig. 9(b)], which

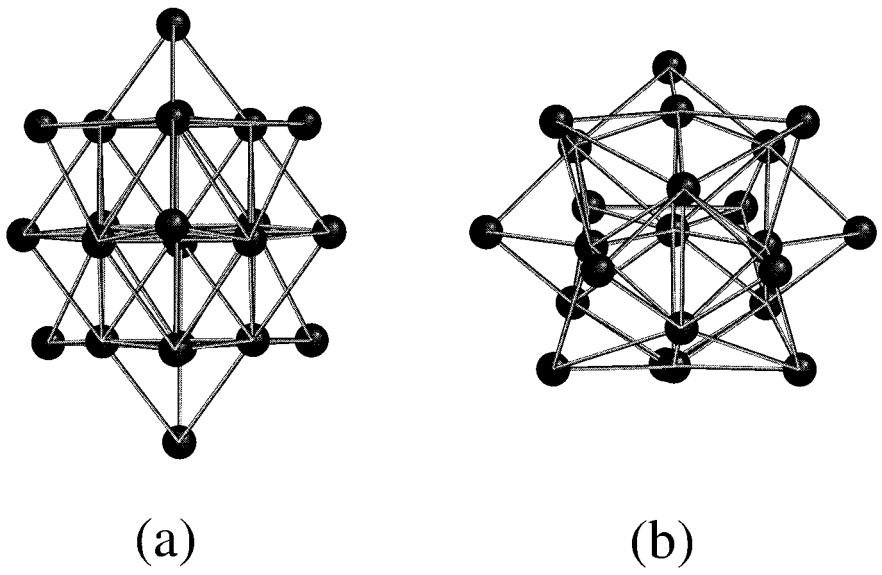

FIG. 6. The relaxed configurations for the (a) fcc and (b) IC1 Ni_{23}.

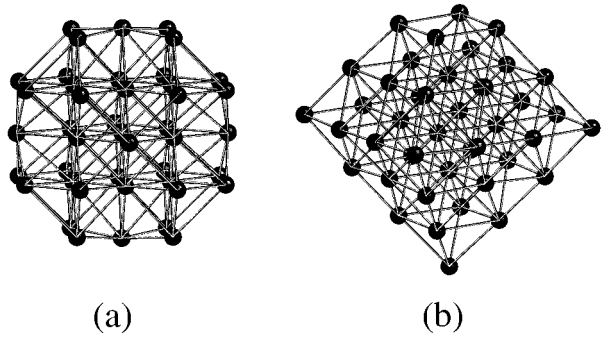

FIG. 8. Two relaxed fcc geometries for $n=43$. (a) A geometry consisting of a central atom and its neighbors up to the third shell. (b) A geometry produced by the removal of an apex atom from the 44-atom multioctahedral structure.

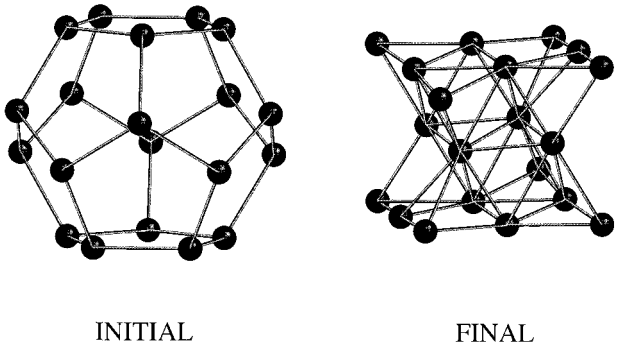

FIG. 10. The initial and final geometries for the Ni_{20} dodecahedral structure.

is also identical to the geometry obtained by adding all the neighbors up to the fourth shell to a Ni_{13} cuboctahedron. The procedure is similar to the way the second Mackay's icosahedron is constructed from the first. We find the IC configuration to be energetically more favorable with binding energy larger than the fcc geometry by 0.17 eV per atom. This comparison is significant since this is the second opportunity for comparing such structures, recalling the first occurring for Ni_{13}. It should be noted that the CO structure is one of the most compact geometries of the fcc types. Both structures, for $n=55$, were found to be devoid of any distortions on relaxation.

Additionally, we also considered two structures other than fcc and icosahedral types for completeness. These structures were found to have lower binding energies per atom, and some of them even unstable. For example, the Ni_{20} dodecahedral structure [Fig. 10] was found to be unstable and relaxed to a fcc-like structure. Finally, we have found that the Ni_{15} bcc cluster, although metastable with significant distortions, had much lower binding energy per atom when compared with other clusters.

In Table IV we give a summary of our results for binding energies and average bond lengths for Ni clusters in the range $10<n\leqslant 55$.

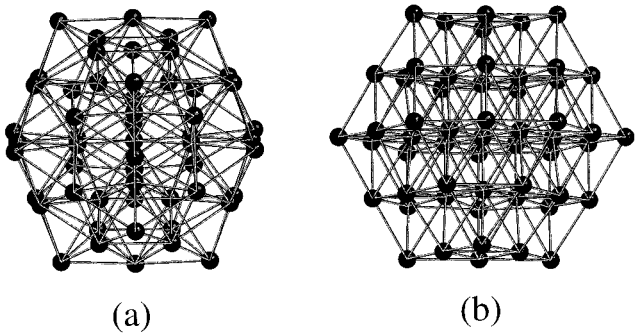

FIG. 9. The relaxed configurations for the (a) icosahedral and (b) the fcc (cuboctahedral) geometries for Ni_{55}.

B. Normal frequencies

The normal frequencies for the clusters $n\leqslant 10$ were obtained by diagonalizing the dynamical matrix D_{ij} of Eq. (15).

For the Ni_2 dimer we obtain $\omega=254$ cm^{-1}, which compares favorably with the experimental value of 330 cm^{-1},

TABLE IV. Binding energies and average bond lengths for Ni clusters in the range $10<n\leqslant 55$.

Number of atoms	Structure	Binding energy per atom (eV)	Average bond length (Å)
13	icosahedral[a]	3.16	2.57
13	fcc[f,h]	2.73	2.48
14	fcc[g]	3.01	2.49
15	bcc[f]	3.04	2.52
19	icosahedral[b,c]	3.33	2.55
19	icosahedral[b,d]	3.28	2.58
19	icosahedral[c,e]	3.32	2.58
19	fcc[f,i]	3.41	2.52
23	icosahedral[b,c]	3.36	2.55
23	fcc[g]	3.43	2.55
24	icosahedral[b,d]	3.50	2.56
24	fcc	3.55	2.56
26	fcc	3.59	2.56
33	icosahedral[a,e]	3.82	2.61
38	icosahedral[b,d]	3.77	2.58
38	fcc[h]	3.94	2.55
43	fcc[f]	3.83	2.55
43	fcc[j]		
44	fcc[i]	3.98	2.55
55	icosahedral[a]	4.27	2.59
55	fcc[f,h]	4.10	2.56
bulk	fcc	4.44	2.50

[a]Full icosahedral geometry.
[b]Open icosahedral geometry.
[c]IC1 type of icosahedral geometry (Ref. 7).
[d]IC2 type of icosahedral geometry.
[e]Twin-icosahedral geometry (Ref. 36).
[f]Central atom with first, second, third, and fourth neighbors correspondingly.
[g]One, two, etc. conventional cells with a common face.
[h]Truncated octahedron (cuboctahedron).
[i]Multioctahedron.
[j]Multioctahedron with the removal of one atom.

TABLE V. Normal vibrational frequencies for Ni_n clusters with $n \leqslant 10$ using the present method.

Number of atoms	Frequencies (cm^{-1})
2	254
3	265, 193, 193
4	232, 225, 225, 224, 75, 20
5	241, 202, 202, 201, 116, 86 37, 37, 37
6	243, 184, 184, 182, 150, 103 86, 51, 23, 23, 22, 22
7	240, 194, 166, 152, 144, 136, 117, 113, 66, 47, 45, 35, 33, 3
8	247, 232, 217, 191, 173, 151, 137, 137, 120, 103, 92, 81, 65, 53, 42, 32, 22, 3
9	256, 243, 226, 204, 196, 188, 176, 163, 136, 134, 125, 123, 117, 101, 91, 78, 69, 62, 56, 48, 37
10	247, 228, 220, 200, 200, 191, 169, 160, 150, 141, 137, 129, 114, 104, 98, 94, 83, 78, 75, 70, 63, 60, 54, 50

and within the range of reported theoretical *ab initio* values (between 190 and 289 cm^{-1}, quoted in Ref. 19).

In Table V we present our calculated normal vibrational frequencies for the Ni_n clusters with $n \leqslant 10$. Unfortunately, we were not able to find experimental values (for $n \geqslant 3$) for comparison, and therefore our results should be taken as predictions for future experimental findings.

C. Ionization energies

As pointed out in Sec. II D, the present formalism can be relied on to give only qualitative results on the variation of the ionization energy with cluster size. In Table VI we present our results for Ni_n clusters with $n \leqslant 7$. From these results it is clear that in accordance with the experimental results, the ionization energy exhibits a dip for Ni_5 and an increase for Ni_6, followed by a smaller dip for Ni_7. For Ni_4, however, both the present results and those of Ref. 26 indicate an increase in the ionization potential relative to that for Ni_5, a trend in opposition to the experimental results.[8,7]

TABLE VI. Ionization energies of small Ni_n clusters, $n \leqslant 7$. A constant shift in the energies was needed for making direct comparison.

	Ionization energies (eV)		
n	Present work	Expt.	Ref. 26 (theory)
3	7.18		
4	7.13	5.66[a]	6.08
5	6.73	6.17[a]	5.83
6	6.80	6.80[b]	6.29
7	6.79	6.07[a]	5.89

[a]Reference 8.
[b]Reference 7.

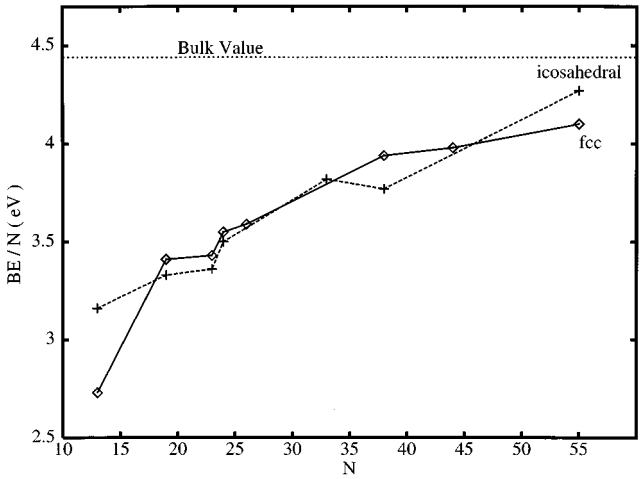

FIG. 11. The dependence of the binding energy per atom with cluster size for icosahedral and fcc structures.

IV. CONCLUSION

The present investigation on Ni_n clusters with $n \leqslant 55$ leads us to some important conclusions regarding their properties. In particular, our results show the closed icosahedral structures to be energetically more favorable for cluster formation in the range considered (Fig. 11). This is in agreement with the experimental findings of Parks *et al.*,[7,11] although their evidence for cluster structures for this size regime were not strongly conclusive.

It seems that the weak d-orbital effects are not strong enough to prevent IC packing in Ni, which is the norm for almost all spherically symmetric interactions, e.g., clusters of noble gases. Among transition metals, Ni has the least d-orbital dependence. This conclusion comes from the fact that in our model the strength of $d-d$ interaction depends on the value of the parameter r_d [see Eq. (2)]. As we see in the Solid State Table of Ref. 37, Ni has the lowest value of r_d for any of the transition metals. Indeed, if some of the transition metals were to prefer IC packing, Ni should be among them. The open IC structures, on the other hand, were found to be less favorable compared to octahedral (fcc)-type structures (Fig. 11). The most stable structures among the fcc geometries appear to be the truncated octahedra (cuboctahedra), like Ni_{13}, Ni_{38}, Ni_{55}, the multioctahedra like Ni_{19} or Ni_{44}. The twin-icosahedral structures seems to be energetically equivalent compared with the IC2 type of icosahedral packing, with the closed twin-icosahedral configuration for $n=33$ being very stable.

From the results shown in Table IV we can see that trends for the binding energy per atom and the average bond length with the increase in the cluster size are well described. The binding energy increases, although not monotonically, with the cluster size. On the other hand, the average bond length decreases with the cluster size. These tendencies are

not monotonic, because of the different ways of constructing various isomers for each n. The increase in binding energy per atom with the cluster size reflects, in part, the many-body character of the interactions and, in part, the surface effects in the crystal formation. This is also seen in the variation of the average bond length, which for most of the structures studied is larger than that of the bulk. This is due to the relatively large ratio of surface atoms to bulk atoms. The surface atoms are less tightly bound, causing an increase in the average bond length.

Our results for the optimum cluster geometries, the variation of the binding energy, and the average bond length with the cluster size, as well as the normal vibration frequency of the dimer, are in good quantitative agreement with both theory and experiment. On the other hand, the present approach fails to reproduce quantitative results for ionization energies, due mainly to the pure scaling of the SK-TB parameters with the local (lattice) field or, equivalently, due to the poor fitting of the SK-TB parameters to small clusters. In our method this drawback is offset by fitting our total interaction potential to the experimental bond length of the dimer. This is why our results for the cluster properties that depend on the total energy (and not merely only on its electronic part) agree quantitatively with experiment. These observations bring up two questions: namely that of the proper scaling of the SK-TB parameters and that related to the level of the *ab initio* character, that the present calculational scheme can acquire.

The first question is currently being examined by implementing scaling schemes for the SK-TB parameters within the present formalism by allowing one to take into account the local field effects accurately.[40] The second question is related to the possibility of employing scaling schemes for the SK-TB parameters, which are based on a firm *ab initio* footing. This requirement seems to be answered by the recently proposed scaling scheme of Cohen, Mehl, and Papaconstantopoulos[42] provided that their scheme could be suitably extended to include the treatment of small clusters. This is a necessary condition in order to eliminate any deficiencies related to the first question. It has to be kept in mind, however, that the required scaling should be simple enough and computationally efficient in order to allow its use in simulations involving a large number of particles.

In conclusion, we have demonstrated the applicability of our TBMD calculational scheme by doing a systematic study of TMCs and emphasized the limitations of its present form. At the same time, we have also discussed the possibilities for improvement of the present theory in order that it acquire *ab initio* character, in contradistinction to its present semiempirical nature. Thus, the proposed calculational scheme for transition metal clusters, following earlier successful applications on semiconductors[1] offers a theoretical approach to both covalent and metallic systems at a multilevel description, ranging from a semiempirical one to that exhibiting a firm *ab initio* character. The level of accuracy of the method to be used depends on the requirements of the user. Due to its computational efficiency, the present method can serve as an efficient tool for studying complex systems for which *ab initio* methods are not easily applicable.

ACKNOWLEDGMENTS

The present work is supported by the European Community Grant No. ECUS-007-9825, National Science Foundation Grant No. EHR 91-08764, and the University of Kentucky Center for Computational Sciences.

[1] M. Menon and R. E. Allen, Phys. Rev. B **33**, 7099 (1986); **38**, 6196 (1988).
[2] M. Menon and K. R. Subbaswamy, Phys. Rev. B **47**, 12 754 (1993).
[3] P. Ordejòn, D. Lebedenko, and M. Menon, Phys. Rev. B **50**, 5645 (1994).
[4] M. Menon and K. R. Subbaswamy, Phys. Rev. B **50**, 11 577 (1994).
[5] M. Menon, K. R. Subbaswamy, and M. Sawtarie, Phys. Rev. B **49**, 13 966 (1994).
[6] M. Menon and K. R. Subbaswamy, Phys. Rev. B **51**, 17 952 (1995).
[7] E. K. Parks, B. J. Winter, T. D. Klots, and S. J. Riley, J. Chem. Phys. **94**, 1882 (1991).
[8] M. B. Knickelbein, S. Yang, and S. J. Riley, J. Chem. Phys. **93**, 94 (1990).
[9] F. Liu, M. R. Press, S. N. Khanna, and P. Jena, Phys. Rev. B **38**, 5760 (1988).
[10] G. Apai, J. F. Hamilton, J. Stohr, and A. Thompson, Phys. Rev. Lett. **43**, 165 (1979).
[11] M. Pellarin, B. Baguenard, J. L. Vialle, J. Lerme, M. Broyer, J. Miller, and A. Perez, Chem. Phys. Lett. **217**, 349 (1994).
[12] T. D. Klots, B. J. Winter, E. K. Parks, and S. J. Riley, J. Chem. Phys. **92**, 2110 (1990).
[13] G. D'Agostino, Philos. Mag. B **68**, 943 (1993).
[14] Ph. Buffat and J. P. Borel, Phys. Rev. A **13**, 2287 (1976).
[15] T. Kastro, R. Reifenberger, E. Choi, and R. P. Andres, Surf. Sci. **234**, 94 (1990).
[16] B. Moraweck, G. Clugnet, and A. J. Renouprez, Surf. Sci. **81**, L631 (1979).
[17] T. P. Martin, U. Näher, T. Bergmann, H. Göhlich, and T. Lange, Chem. Phys. Lett. **183**, 119 (1991).
[18] T. P. Martin, T. Bergmann, H. Göhlich, and T. Lange, Chem. Phys. Lett. **176**, 343 (1991).
[19] H. Basch, M. D. Newton, and J. W. Moskowitz, J. Chem. Phys. **73**, 4492 (1980).
[20] M. Tomonari, H. Tatewaki, and T. Nakamura, J. Chem. Phys. **85**, 2875 (1986).
[21] P. Mlynarski and D. R. Salahub, J. Chem. Phys. **95**, 6050, (1991).
[22] O. Gropen and J. Almlof, Chem. Phys. Lett. **191**, 306 (1992).
[23] N. Rösch, L. Ackerman, and G. Paccioni, Chem. Phys. Lett. **199**, 275 (1992).
[24] S. Valkealahti and M. Manninen, Comput. Mat. Sci. **1**, 123 (1993).
[25] A. Kant, J. Chem. Phys. **41**, 1872 (1964).
[26] M. A. Nygren, P. E. M. Siegbahn, U. Wahlgren, and H. Akeby, J. Phys. Chem. **96**, 3633 (1992).
[27] J. L. Chen, C. S. Wang, K. A. Jackson, and M. R. Pederson, Phys. Rev. B **44**, 6558 (1991).
[28] Z. Yu and J. Almlöf, J. Phys. Chem. **95**, 9167 (1991).
[29] C. L. Cleveland and U. Landman, J. Chem. Phys. **94**, 7376 (1991).
[30] S. Valkealahti and M. Manninen, Phys. Rev. B **45**, 9459 (1992).
[31] M. Menon, J. Connolly, N. Lathiotakis, and A. N. Andriotis, Phys. Rev. B **50**, 8903 (1994).
[32] N. N. Lathiotakis, A. N. Andriotis, M. Menon, and J. Connolly, Europhys. Lett. **29**, 135 (1995).
[33] A. L. Mackay, Acta Crystallogr. **15**, 916 (1962).
[34] See, for example, L. D. Marks, Philos. Mag. A **49**, 81 (1984).
[35] See, for example, B. Rault, J. Farges, M. F. De Feraudy, and G. Torchet, Philos. Mag. B **60**, 881 (1989).
[36] J. Farges, M. F. de Feraudy, B. Rault, and G. Torchet, J. Chem. Phys. **84**, 6 (1986).
[37] W. Harrison, *Electronic Structure and the Properties of Solids* (Freeman, San Francisco, 1980).
[38] J. C. Slater and G. F. Koster, Phys. Rev. **94**, 1498 (1954).
[39] N. Lathiotakis and A. N. Andriotis, Solid State Commun. **87**, 871 (1993).

[40] A. N. Andriotis, J. Phys. Condensed Matter **7**, L61 (1995).
[41] D. Tomanèk and M. Schluter, Phys. Rev. B **36**, 1208 (1987).
[42] R. E. Cohen, M. J. Mehl, and D. A. Papaconstantopoulos, Phys. Rev. B **50**, 14 694 (1994).
[43] D. A. Papaconstantopoulos, *Handbook of the Band Structure of Elemental Solids* (Plenum, New York, 1986).
[44] V. L. Moruzzi, J. F. Janak, and A. R. Williams, *Calculated Electronic Properties of Metals* (Pergamon, New York, 1978).